Journal of Power Sources, 2 (1977/78) 369 - 385

PASSIVATION REACTIONS ON THE ELECTRODES OF A LEAD–ACID CELL

A. WINSEL, U. HULLMEINE and E. VOSS

Varta Batterie AG, Forschungs- und Entwicklungszentrum, Kelkheim/Ts. (F.R.G.)

(Received November 5, 1977; in revised form January 28, 1978)

Summary

The behaviour of Pb and PbO_2 electrodes at high rate low temperature discharges has been investigated. Based on the solution/precipitation model of Vetter it is assumed that the capacity is limited by a diffusion process of the $Pb^{2+}(PbSO_4)$ species away from the current producing internal surface of the electrode through the $PbSO_4$ diaphragm (lead sulphate passivation). From this assumption it can be derived that the capacity of an electrode having a small surface area and a large pore volume per unit weight, is proportional to the square of the surface area. This is true for negative electrodes, in particular when discharged in electrolytes of high concentration. The high rate low temperature capacity of electrodes with large surface areas, *e.g.* of positive electrodes, is determined by the pore volume of the active material. This may also be valid for negative electrodes, especially when discharged in electrolytes of low concentration. Again the $Pb^{2+}(PbSO_4)$ diffusion through a diaphragm of reaction products is limiting the capacity. However, contrary to pure $PbSO_4$ passivation the diaphragm now consists of $PbSO_4$ and ice crystals. These are formed due to the isothermal dilution of the pore liquid as soon as its concentration coincides with the solidus curve of the H_2SO_4/H_2O phase diagram (ice passivation).

Introduction

The behaviour of a lead–acid cell at high rates of discharge is of importance for automotive as well as for electric vehicle batteries. Generally two processes are considered to be responsible for the voltage decay at the end of discharge: increasing deficiency of sulphuric acid in the pores of the active material, and the formation of a passivating $PbSO_4$ layer [1, 2]. A number of investigations have been performed to decide whether the formation of $PbSO_4$ during discharge occurs by a solid state reaction or via a solution/precipitation mechanism [3 - 5]. As will be shown in this work, the capacity limiting processes on the negative and positive electrode can be quantitatively understood on the basis of Vetter's solution/precipitation

mechanism [6], especially at high rates and low temperatures. Conditions of this nature are of significance for the so-called low temperature cranking capability of SLI batteries as specified in European and U.S. specifications.

Theoretical considerations

During the discharge of an electrode passivating layers of $PbSO_4$ are formed by a solution/precipitation mechanism. It is evident from the SEM pattern that these layers form a diaphragm consisting of an accumulation of mostly well defined $PbSO_4$ crystals. This diaphragm is a transport barrier which may have the following effects [7]: the diaphragm contributes merely to the internal resistance; the diaphragm inhibits the diffusion of HSO_4^- species to the surface of the lead electrode where it is used for the formation of additional $PbSO_4$; the $PbSO_4$ formed at the surface has to be transfered through the diaphragm away from the surface. The solubility of $PbSO_4$ is highest at the surface and lowest outside the diaphragm. Consequently, there is a tendency for $PbSO_4$ (Pb^{2+}) species to migrate through the diaphragm and to crystallize at the diaphragm/electrolyte interface.

It can be shown by simple considerations that the contribution of the diaphragm to the internal resistance must be insignificant. The resistance R_δ of the diaphragm of thickness δ is given by:

$$R_\delta \approx \frac{\rho \cdot \delta \cdot \lambda}{S \cdot P^*} \tag{1}$$

and since δ is very small and the internal surface S very high, R must be small even at low porosities P^*. Therefore, the diaphragm resistance cannot be a limiting factor.

Also the diffusion of HSO_4^- species to the electrode surface cannot be rate limiting if compared to the $PbSO_4$ (Pb^{2+}) diffusion away from the surface. There is a difference in the concentration of these two species of about 10^6, *i.e.* the H_2SO_4 concentration is, under conditions usually prevailing in a lead–acid cell, 10^6 times higher than the $PbSO_4$ concentration. Correspondingly, the H_2SO_4 (HSO_4^-) diffusion current is expected to be much higher than the $PbSO_4$ diffusion current. Therefore, we assume that the diffusion of $PbSO_4$ (Pb^{2+}) species away from the electrode surface through the $PbSO_4$ diaphragm is the rate and capacity determining process during discharge. The thickness of this diaphragm increases during discharge to such an extent that finally due to a high supersaturation at the surface spontaneous precipitation of $PbSO_4$ occurs thus producing a rapid voltage decay which indicates the end of discharge.

Pore structure and passivation layer

We assume that the distribution of pore surface and volume of the active material according to their radii are known. Then by equation:

$$O(r)\,\mathrm{d}r = 2\pi r l(r)\,\mathrm{d}r \tag{2}$$

the internal surface (cm^2/g) is given by the pores having radii between r and $r + dr$. Correspondingly, we obtain the distribution of pore volumes:

$$V(r)\,dr = \pi r^2 l(r)\,dr \tag{3}$$

giving us the pore volume (cm^3/g), $l(r)\,dr$ being the total length of all pores between r and $r + dr$. The ratio of these two distribution functions is given by:

$$\frac{V(r)}{O(r)} = \frac{r}{2} \tag{4}$$

For a mathematical treatment we postulate that: the current density at the internal surface is uniform and independent of the pore radius; volume changes occurring during charge/discharge are called ΔV_0; the pores are filled by the reaction products. The original internal surface contributes to the current as long as the pore is not filled completely.

If r_t is the radius of pores which are just being filled entirely at the time t, and hence do not contribute to the current any more, we calculate the current density to be:

$$j = \frac{I}{\int_{r_t}^{\infty} O(r)\,dr} \tag{5}$$

I is the current and the integral represents the total internal surface available at the time t. The remaining pore volume can be calculated from the original pore volume and the volume of the solid reaction products formed in the pores:

$$V(r,t)\,dr = V(r)\,dr - \Delta V_0 O(r)\,dr \int_0^t j(\tau)\,d\tau \tag{6}$$

The term $\Delta V_0 O(r)\,dr \int_0^t j(\tau)\,d\tau$ comprises the total volume change produced by the charge applied to the electrode. If $V(r_t, t) = 0$, all pores having a radius smaller than r_t are filled and no longer contribute to the current. Therefore,

$$V(r_t) = \Delta V_0 O(r_t) \int_0^t j(\tau)\,d\tau \tag{7}$$

and using eqn. (5), we obtain

$$\Delta V_0 I \int_0^t \frac{d\tau}{\int_{\tau}^{\infty} O(r)\,dr} = \frac{V(r_t)}{O(r_t)} = \frac{r_t}{2} \tag{8}$$

Differentiation of eqn. (8) gives:

$$2\Delta V_0 I = \left(\frac{dr_t}{dt}\right) \int_{r_t}^{\infty} O(r)\,dr \tag{9}$$

and integration of eqn. (9) again, results in:

$$2\Delta V_0 It = \int_0^{r_t} \left[\int_{r_\tau}^{\infty} O(r)\,dr\right] dr_\tau \tag{10}$$

In eqn. (10) for a given function $O(r)$ the value of the integral is a function of r_t and *vice versa*, at a given current I and known ΔV_0 value the radius r_t is a function of time t. Consequently, eqn. (10) describes the time t at which pores of the radius r_t are unable to contribute any longer to the current.

In accordance with our hypothesis of the rate determining diffusion of $PbSO_4$ (Pb^{2+}) a porous $PbSO_4$ layer having a thickness δ is formed in front of the electrode surface. If Δc is the maximum possible concentration gradient for $PbSO_4$ supersaturation, the current density j can only be maintained as long as the reaction product ($PbSO_4$) can diffuse away from the electrode surface and hence:

$$j \leqslant \frac{FP^*D\Delta c}{\lambda \delta_t} \tag{11}$$

with P^* = porosity of the $PbSO_4$ layer, δ_t = thickness of the $PbSO_4$ layer at time t, λ = tortuosity factor, F = Faraday constant, D = diffusion coefficient.

The thickness of the $PbSO_4$ layer at time t is given by:

$$\delta_t = \frac{\Delta V_0}{P^*} \int_0^t j(\tau)\,d\tau \tag{12}$$

Equation (11) very clearly shows that at a constant current, the current producing process cannot be maintained because the transport rate of the $PbSO_4$ (Pb^{2+}) species is decreasing and finally collapsing due to the increase of layer thickness and of current density on the remaining electrode areas. Consequently, as soon as in eqn. (11) the sign of equality is valid, the voltage decay occurs and terminates the electrode capacity.

From eqns. (11), (12), and (5) the following relationship can be derived:

$$\Delta V_0 \int_0^{t^*} \frac{I}{\int_{r_\tau}^{\infty} O(r)\,dr}\,d\tau = \frac{P^{*2}FD\Delta c^*}{\lambda I} \int_{r_t^*}^{\infty} O(r)\,dr \tag{13}$$

At time t^* the end of discharge occurs due to passivation. Combining eqns. (8) and (13), we obtain:

$$\int_{r_t^*}^{\infty} O(r)\,\mathrm{d}r = \frac{\lambda I}{2P^{*2}FD\Delta c^*}\, r_t^* \tag{14}$$

If we know the pore size distribution function, we are able to calculate the pore radius r_t^*, and it is evident that pores having radii smaller than r_t^* are being completely filled with $PbSO_4$ during high rate discharge. The discharge time t^* can be obtained from eqns. (10) and (14):

$$t^* = \frac{1}{2I\Delta V_0} \int_0^{r_t^*} \left[\int_{r_\tau}^{\infty} O(r)\,\mathrm{d}r \right] \mathrm{d}r_\tau \tag{15}$$

This equation also gives information on the high rate capacity $I \cdot t^*$. If the total internal surface of the active material (cm^2/g) is given by:

$$S = \int_0^{\infty} O(r)\,\mathrm{d}r \tag{16}$$

we obtain from eqn. (15) after some calculations the result:

$$It^* = \frac{1}{\Delta V_0} \left\{ \left[S - \int_0^{r_t^*} O(r)\,\mathrm{d}r \right] \frac{r_t^*}{2} + \int_0^{r_t^*} V(r)\,\mathrm{d}r \right\} \tag{17}$$

If there is no microporosity in the active material, *i.e.* no pores are completely filled with $PbSO_4$ during a high rate discharge, the electrode behaves similarly to a sheet of lead or lead dioxide. Under this condition the current density j remains constant and from eqns. (5), (11), and (12) a simple relationship can be derived:

$$\frac{I^2 t^*}{S^2} = \frac{FP^{*2}D\Delta c}{\lambda \Delta V_0} = K \tag{18}$$

As can be seen from eqn. (18), the capacity especially at high rates is proportional to the second power of the internal surface of the active material, and inversely proportional to the current, provided that the P^* and λ values characteristic of the $PbSO_4$ layer do not change very much. The effect of temperature on the high rate capacity mainly depends on its effect on the diffusion coefficient D and the concentration of a supersaturated $PbSO_4$ solution Δc. However, if there is a microporosity as is normally the case in positive active material, we have to rely upon eqn. (17). This equation informs us that the high rate capacity of an electrode is exhausted as soon as the internal surface is covered by a $PbSO_4$ layer having a thickness of $\delta^* = r_t^*/2$. The term $S - \int_0^{r_t^*} O(r)\mathrm{d}r$ describes the surface area of pores having a radius greater than r_t^*. Pores having a radius smaller than r_t^*, contribute with their volume as expressed by the term $\int_0^{r_t^*} V(r)\mathrm{d}r$ in eqn. (17).

Equations (17) and (18) can be checked experimentally. The value of r_t^* may be determined from experiments on smooth sheet electrodes. Since the internal parameters of porous electrodes, such as surface area and pore size and volume distribution, can be measured by independent procedures, it is possible to relate the results of experiments on smooth and porous electrodes to each other.

Capacity limitation by electrolyte deficiency

Lead sulphate passivation as we call the type of capacity limiting process discussed so far, can only occur as long as sufficient acid is made available in the pores either by diffusion or convection or by forced flow of electrolyte. If this is not the case, the capacity is determined by the amount of electrolyte or limited by electrolyte deficiency. Under these conditions the capacity at a high rate discharge C_H is given by:

$$C_H = 2\kappa F V_p \Delta m \tag{19}$$

with F = Faraday constant, V_p = pore volume of active material (cm^3/g), Δm = available amount of acid per volume of initial electrolyte, κ = a factor close to unity which takes into account transference and diffusion of H_2SO_4 from outside the pore system. The value of Δm can be calculated easily if the sum of the partial molar volumes of the substances involved in the electrode reactions is assumed to be constant. Since by the reaction on the negative electrode only H_2SO_4 is consumed whereas the amount of H_2O remains unchanged, we obtain:

$$\Delta m_- = m^0 \frac{y^0 - y^1}{1 - y^1} \tag{20}$$

By analogy with this procedure we obtain the equation for the positive electrode:

$$\Delta m_+ = m^0 \frac{y^0 - y^1}{1 + y^1} \tag{21}$$

which indicates that while H_2SO_4 is consumed, H_2O is formed simultaneously as is generally known from the corresponding equation of the electrode reaction.

Ice passivation due to electrolyte deficiency

As long as we discharge a lead–acid cell at temperatures higher than 0 °C, the final concentration of the electrolyte (x^1, y^1) is attained at the moment of insufficient electrolytic conductivity in the pores. As a first approximation this may be valid for $y^1 \cong 0$. At temperatures lower than 0 °C, however, this is not correct any more. The final electrolyte concentration now is defined by its freezing point.

As is obvious from Fig. 1, showing a part of the H_2SO_4/H_2O phase diagram, we move from the point y^0 to the point y^1 while a lead–acid cell is discharged at −18 °C. As soon as we proceed (or discharge) further, ice

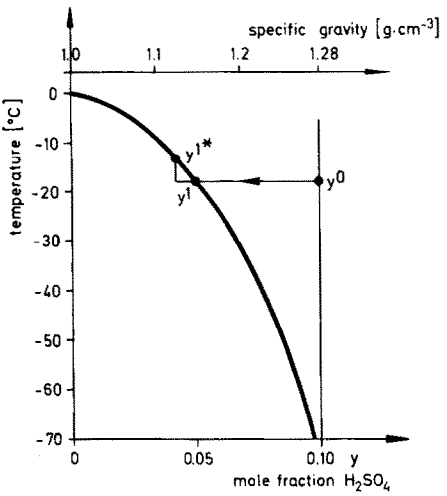

Fig. 1. Lower end section of the H_2SO_4/H_2O phase diagram.

crystals are formed which are deposited on the internal surface of the electrode material as a diaphragm showing exactly the same effect as the $PbSO_4$ layer discussed earlier. This process which we call ice passivation, is responsible for the voltage decay and capacity limitation at the end of a high rate low temperature discharge.

From eqn. (18) the capacity $C_H = I \cdot t^* \equiv C_{HS}$ limited by $PbSO_4$ passivation can be calculated:

$$C_{HS} = K \frac{S^2}{I} \tag{22}$$

The subscript S indicates that the internal surface S of the active material is controlling the capacity. On the other hand the capacity $C_H = I \cdot t \equiv C_{HV}$ limited by ice passivation, is derived from eqn. (19):

$$C_{HV} = 2\kappa F V_p \Delta m \tag{23}$$

The subscript V indicates that the pore volume is controlling the capacity.

It is evident that at a certain specific point depending on the internal parameters, $PbSO_4$ passivation should change over to ice passivation and *vice versa*. At this point C_{HS} and C_{HV} are expected to be equal and we obtain a critical factor f^*:

$$f^* = \frac{V_p}{S^2} = \frac{K}{2\kappa F I \Delta m} \tag{24}$$

Once we have determined f^* experimentally, we are in the position to decide from simple measurements of the two internal parameters V_p and S of the active material whether $PbSO_4$ or ice passivation will take place at a given temperature, electrolyte concentration, and current density.

Experimental

The capacity measurements on the electrodes of conventional SLI type were performed in a specially designed cell having excess electrode capacity of opposite polarity. The electrolyte temperature was kept constant at −18 °C. The electrolyte concentration was kept constant at a pre-chosen level throughout each discharge by circulation from a reservoir. Discharges were performed at constant current, electrode potentials were followed by applying Hg/Hg_2SO_4 reference probes at different sites on the electrode. In the case of capacity measurements the cut-off voltage was 0 V *versus* Hg/Hg_2SO_4 in the same electrolyte. The surface of the active material was determined by a conventional BET method, pore volume, and pore size distribution by means of a Hg porosimeter. To prevent amalgamation of the negative active material, the Pb surface has been sulphidized, *i.e.* a PbS layer has been formed prior to the measurements.

Results and Discussion

Potential–time curves at constant current discharge

Figure 2 shows typical potential–time curves of two different negative electrodes (curves 1 and 2) and of one positive electrode (curve 3) obtained at a discharge rate of 150 mA/cm^2 at −18 °C. As can be seen, the negative electrode represented by curve 1 exhibits a rapid transition to the PbO_2/$PbSO_4$ potential (point A). The behaviour is typical for electrodes having a low internal surface area, and in accordance with the previous theoretical consideration the capacity of this electrode is limited by $PbSO_4$ passivation. Contrary to electrode 1, the electrode represented by curve 2 has a high surface area. Its potential–time curve shows a broad range of transition (point B) which is typical for electrodes limited by ice passivation. Ice

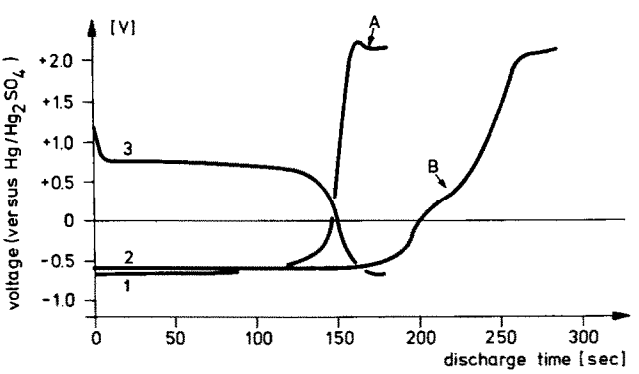

Fig. 2. Potential–time curves of positive and negative electrodes at −18 °C and 150 mA/cm^2 constant current discharge. 1, negative electrode with $PbSO_4$ passivation; 2, negative electrode with ice passivation; 3, positive electrode.

passivation is unstable by nature *versus* H_2SO_4 diffusion and temperature increase, and the competition between these two processes and the ice formation may explain the typical behaviour.

In positive electrodes (curve 3) normally ice passivation is the capacity limiting process due to the high surface area of their active material (see below). Therefore, the range of transition is again relatively broad.

Capacity as a function of surface area

As pointed out earlier, the simple eqn. (18) is valid only as long as there is no microporosity, *i.e.* pore radius smaller than r_t^*. This postulate has been checked experimentally for negative active material by determining the nitrogen sorption isotherm. As can be seen from Fig. 3, no hysteresis is observed between the adsorption and desorption isotherms. Consequently, there are no pores smaller than 500 Å in diameter in the negative active material. This is confirmed further by the correlation of results obtained by mercury porosimetry (R) and BET surface area measurements (S). From Fig. 4 it is evident that there is a linear relationship between R and S the line going through the origin. Values of R have been calculated from the pore size distribution curves by using the equation:

$$R = \int_0^\infty \frac{2}{r}\, dV(r) \tag{25}$$

As we have learned from eqn. (22), the capacity of an electrode should be

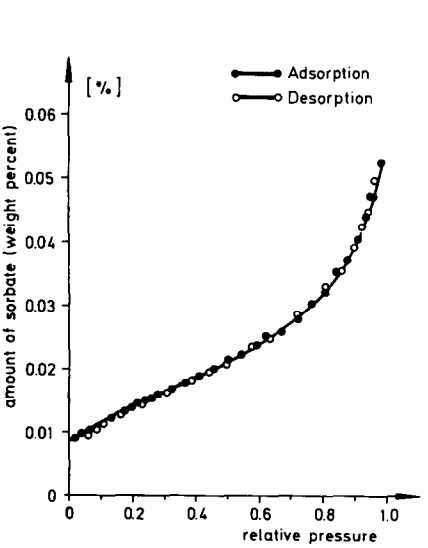

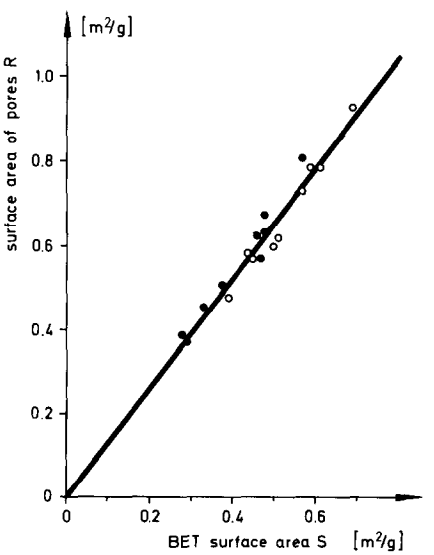

Fig. 3. Sorption isotherm of formed negative active material.

Fig. 4. Correlation between surface area R calculated from the pore size distribution, and experimental BET surface area S.

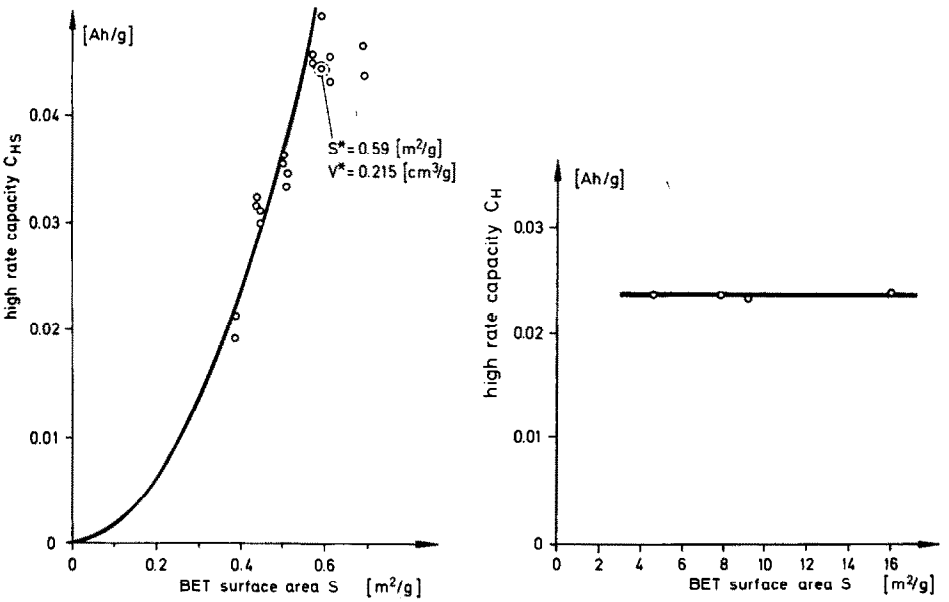

Fig. 5. High rate capacity (150 mA/cm^2) of negative electrodes obtained at −18 °C as a function of surface area of the negative active material. ——, Calculated from eqn. (22); ○, experimental values.

Fig. 6. High rate capacity of positive electrodes obtained at −18 °C as a function of surface area of positive active material.

proportional to S^2 as long as $PbSO_4$ passivation occurs. To check this relationship we have prepared a series of electrodes having different specific surface areas but constant pore volume. The results of capacity measurements at −18 °C and j = 150 mA/cm^2 obtained on these electrodes are given in Fig. 5.

It is evident from this diagram that most of the experimental points fit quite well to the curve (solid line) calculated from eqn. (22). A group of points, however, shows considerably lower capacity than expected. A detailed analysis of these points indicates that for these electrodes eqn. (22) is not valid because not $PbSO_4$ passivation but ice passivation had occurred. If we take, for instance, the characteristic values of one of these points (marked by a circle) which is lying on the borderline, and calculate a critical factor f^*, we obtain $f^* = 0.62 \times 10^{-8}$ g/cm, using S = 0.59 m^2/g, and V = 0.215 cm^3/g.

Positive active material generally shows a surface area ten times as high as that of negative material. Therefore, positive electrodes normally show ice passivation only. If this is correct no effect of the surface area of the positive active material on the capacity should be expected. In Fig. 6 we have plotted capacity data obtained on positive electrodes (−18 °C; 150 mA/cm^2) *versus* the BET surface of positive active material. As can be seen, there is no effect of surface area at all. We know, however, from earlier measurements that the

capacity of positive electrodes strongly depends on the pore volume of the positive active material, and this indeed agrees very well with the occurrence of ice passivation at positive electrodes.

Capacity as a function of acid concentration

It is evident from eqn. (19) that by investigating the capacity C_H of a series of identical electrodes in dependence of Δm, *i.e.* in dependence on the acid concentration, the point should be found where $C_{HV} = C_{HS}$. This again would provide the necessary data to calculate the critical factor f^* by means of eqn. (24).

In Fig. 7 the results of such an investigation are given. In this diagram the capacities of both negative and positive electrodes obtained at −18 °C and 150 mA/cm^2 are plotted *versus* the acid concentration. As can be seen, both curves meet the concentration axis at the same point, namely 2.25 mol/l or $y^{1^*} = 0.042$. This indicates that for both electrodes the limiting process must be the same, namely ice passivation.

Using eqn. (19) and the pore volume data given in Table 1, we are able to calculate the theoretical high rate capacities C_{HV} as a function of the initial acid concentration y^0. As can be seen from Table 1, the calculated values C_{HV} are lower than the experimental data C_H. From this deviation the values of κ can be calculated by:

$$\kappa = \frac{C_H}{C_{HV}} \tag{26}$$

Again from Table 1 it is evident that κ is a fairly constant value for both negative ($\kappa = 1.45$) and positive ($\kappa = 1.31$) electrodes.

Looking once again at Fig. 7 we find that the curve representing the behaviour of the negative electrode exhibits a maximum at 4.50 mol/l. This

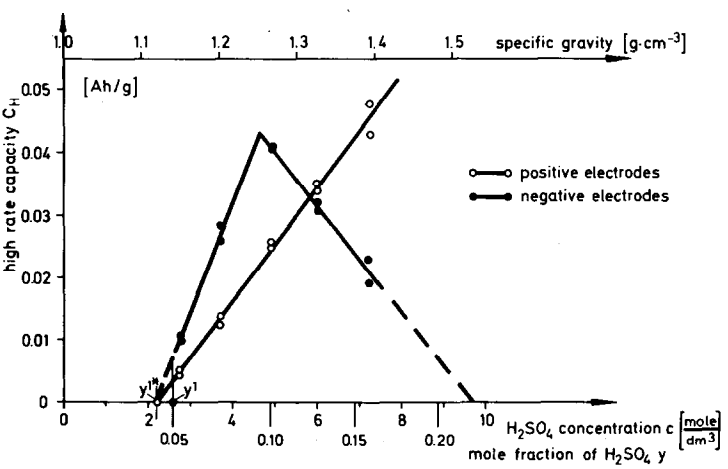

Fig. 7. High rate capacity of positive and negative electrodes (−18 °C) as a function of electrolyte concentration.

TABLE 1

Experimental data and calculation of the high rate low temperature capacities of positive

Gravity of electrolyte 20 °C (g/cm^3)	Concentration of electrolyte $C_{20°C}$ (mol/dm^3)	Total amount of mol H_2SO_4 and H_2O (mol/dm^3)	Mol fraction H_2SO_4 y	Δm_+ (mol/dm^3)	Sp. pore volume V_+ (cm^3/g)	Capacity (150 mA/cm^2, −18 °C) C_{H_+} (Ah/g)	
						Exp.	Exp. from Fig. 7
1.121	2.000	54.283	0.038				
1.135	2.250	53.971	0.042				
1.157	2.623	53.603	0.050				
1.164	2.750				0.125	0.0045	
1.178	3.000	53.166	0.058	0.816			0.0069
1.217	3.699				0.125	0.0129	
1.233	4.000	51.780	0.079	1.839			0.0161
1.265	4.600						
1.280	4.876	50.450	0.099	2.760			0.0242
1.281	4.895				0.125	0.0253	
1.286	5.000	50.280	0.102	2.895			0.0254
1.337	5.977				0.125	0.0345	
1.338	6.000	48.644	0.126	3.922			0.0346
1.389	7.000	47.024	0.152	4.964			0.0438
1.400	7.208				0.125	0.0452	
1.440	8.000	45.364	0.180	6.008			0.0530

point is obviously the transition point where $C_{HV} = C_{HS}$, *i.e.* where the $PbSO_4$ passivation changes to ice passivation and *vice versa*. Using the characteristic data of this point ($\kappa = 1.43$, $F = 26.8$ Ah/mol, $I = 0.758$ Ah/g, $\Delta m = 2.66 \times 10^{-3}$ mol/cm^3, and $K = 0.113 \times 10^{-8}$ A^2h/cm^{-4}) and eqn. (24), we calculate the critical factor to be $f^* = 0.73 \times 10^{-8}$ g/cm, which is very close to the earlier value obtained in a quite different and independent way.

For the calculation of the data collected in Table 1, we have used the acid concentration $y^{1*} = 0.042$ as determined by the point of intersection of both curves with the concentration axis in Fig. 7. This value, however, is not in agreement with the acid concentration $y^1 = 0.050$ taken from the solidus curve of the H_2SO_4/H_2O phase diagram at a temperature of −18 °C (Fig. 1).

This discrepancy may be explained as follows: ice passivation does not occur unless a certain amount of ice is formed. Therefore, the mole fraction y^{1*} is a fictitious value only which results from the partition of the sulphuric acid solution into a frozen portion and a residual portion of pore liquid having the correct concentration of $y^1 = 0.050$. If this is correct, the amount of ice necessary for ice passivation can be calculated by using the values of y^1 and y^{1*} and eqn. (20). We obtain the amount of acid Δm produced by the

and negative electrodes

Capacity calc. C_{HV_+} (Ah/g)	$\kappa_+ = \frac{C_{H_+}}{C_{HV_+}}$	Δm_- (mol/dm^3)	Sp. pore volume V_- (cm^3/g)	Capacity (150 mA/cm^2, −18 °C) C_{H_-} (Ah/g)		Capacity calc. C_{HV_-} (Ah/g)	$\kappa_- = \frac{C_{H_-}}{C_{HV_-}}$
				Exp.	Exp. from Fig. 7		
			0.215	0.0100			
0.0055	1.26	0.845			0.0144	0.0097	1.49
			0.215	0.0269			
0.0123	1.31	1.950			0.0323	0.0225	1.44
					0.0431	0.0301	1.43
0.0185	1.31	2.923					
			0.215	0.0405			
0.0194	1.31						
			0.215	0.0314			
0.0263	1.32						
0.0333	1.32						
			0.215	0.0209			
0.0403	1.32						

transition from y^{1^*} to y^1 (Fig. 1). Multiplication of Δm by x^1/y^1 gives us the amount of ice formed:

$$\Delta m_{ice} = \frac{x^1}{y^1}\Delta m_- = m^0 \frac{x^0}{y^1}\frac{y^1 - y^{1^*}}{1 - y^{1^*}} \tag{27}$$

We further calculate:

$$V^*_{ice} = V_{ice} \cdot V_p \cdot \Delta m_{ice} \tag{28}$$

with V_{ice} = molar volume of ice, and V_p = pore volume, and obtain the ice volume per unit weight of active material.

Using $x^0 = 0.901$, $y^0 = 0.099$, $y^1 = 0.050$, $y^{1^*} = 0.042$, $m^0 = 50.45 \times 10^{-3}$ mol/cm^3, $V_p = 0.215$ cm^3/g, and $V_{ice} = 19.6$ cm^3/mol, the result of this calculation is:

$$V^*_{ice} = 32 \times 10^{-3} \text{ cm}^3/\text{g}$$

Since the internal surface area of the negative active material has been measured as 0.59×10^4 cm^2/g, the thickness of the passivating ice layer is calculated to be:

$$\delta_{ice} = 540 \times 10^{-8} \text{ cm}$$

and the ratio $V^*_{ice}/V_p = 0.15$. It is evident that this thickness and that of a $PbSO_4$ passivating layer are of the same order of magnitude.

As shown in Fig. 7 at very high acid concentrations of about 9 - 10 mol/l the capacity of the negative electrodes approaches the value of zero again. In accordance with our hypothesis this may be explained either by a very low diffusion coefficient for the $Pb^{2+}(PbSO_4)$ diffusion through the $PbSO_4$ layer or by a very low concentration gradient due to low supersaturation. Finally, the curve of Fig. 7 representing the positive electrode behaviour, informs us that there is no $PbSO_4$ passivation at this electrode. In the acid concentration range investigated, we observe ice passivation only. As has been pointed out already, the reason for this is the high internal surface area of the positive active material which is about ten times as high as that of negative active material.

Capacity as a function of current density

As long as $PbSO_4$ passivation is predominant, the capacity is expected to be inversely proportional to the current in accordance with eqn. (22). It will be shown that the same relationship is valid for ice passivation also. In Fig. 8 the capacities of positive and negative electrodes of uniform properties obtained at −18 °C are plotted *versus* the inverse of the discharge current. As can be seen, there is a fairly linear relationship for electrodes of both

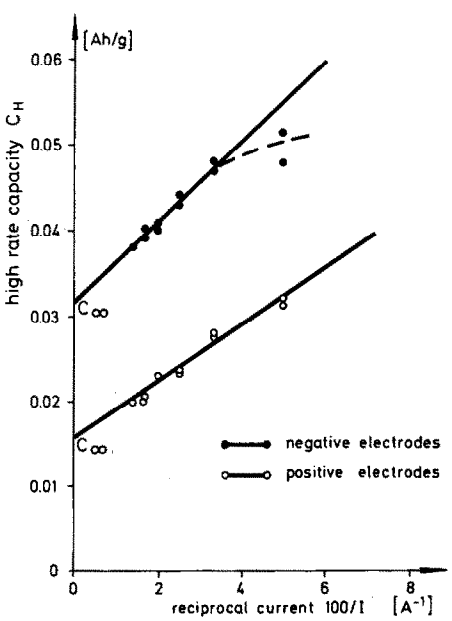

Fig. 8. High rate capacity C_H as a function of the reciprocal of the current.

polarities. This can be explained by a detailed discussion on the mechanism of ice passivation as follows.

During an isothermal discharge at low temperatures the acid is diluted continuously. As soon as the acid concentration coincides with the liquidus curve in Fig. 1, ice crystals are formed having a volume about eight times larger than of the $PbSO_4$ which is generated simultaneously. If we understand the mechanism of ice passivation in this way, we are entitled to assume that the transport processes involved will proceed nearly unaffected down to the "freezing concentration" y^1. We further assume that for $I \Rightarrow \infty$ $(1/I \Rightarrow 0)$, $y^{1^*} \Rightarrow y^1$, *i.e.* ice passivation at $I \Rightarrow 0$ is effected by a zero amount of ice. Under this condition transport of HSO_4^- ions out of the positive electrode ($\kappa_\infty = (1 + n_-)^{-1}$), for instance occurs by transference only while transport by diffusion is zero. The capacity obtainable at a current $I = \infty$ is called C_∞. We define the time $\theta = C_\infty/I$ as a characteristic time for which it is necessary to discharge the electrode with the current I until the first formation of ice crystals (at the concentration y^1, Fig. 1) occurs. From these considerations and from eqn. (23) we derive the relationship:

$$C_\infty = I\theta = 2(1 \overset{+}{(-)} n_-)^{-1} F V_p \Delta m \tag{29}$$

If we now neglect the $PbSO_4$ formed until time θ, we can rearrange eqn. (18) as follows:

$$I^2(t^* - \theta) = KS^2 \tag{30}$$

Since the capacity is defined as $C_H = I \cdot t^*$, we calculate from eqn. (30) the expression:

$$C_H - C_\infty = K\frac{S^2}{I} = C_\infty \frac{I_0}{I} \tag{31}$$

I_0 is a characteristic current, the value of which follows from eqn. (31) to be:

$$I_0 = K\frac{S^2}{C_\infty} \tag{32}$$

Equation (31) describes the behaviour of the high rate capacity as a function of the reciprocal of the current, as shown in Fig. 8. According to this diagram the capacity value for the positive electrode at $1/I = 0$ is $C_\infty = 0.015$ Ah/g. This value has to be compared with the theoretical one which can be calculated from the experimentally determined pore volume of the positive electrode material of $V_p = 0.125$ cm^3/g and a κ_∞-value of:

$$\kappa_\infty = \frac{1}{1 + n_-} = \frac{1}{1.2} = 0.83$$

By using eqns. (19) and (21) we obtain $C_\infty = 0.0155$ Ah/g, which is in good agreement with the value cited above. An analogous calculation can also be made for the negative electrode.

Practical consequences

So far the basic model of $Pb^{2+}(PbSO_4)$ diffusion through the $PbSO_4$/ice layer as a limiting process has been successfully applied to high rate low temperature discharges only. However, from preliminary data we already know that these considerations can be extended to other problem areas also, such as discharge at ambient temperature, discharge under forced flow of electrolyte, and charge acceptance.

The achievements of this work are of immediate practical importance. The quantitative understanding of the cold cranking capability of SLI batteries enables us now: to calculate the cold cranking capacity of electrodes from data obtained by simple physical measurements of some internal parameters (BET surface and pore volume); to design active materials for cold cranking purposes, and to calculate the correct active material balance in a cell; to produce such active materials by choosing and applying the adequate production parameters; to detect and locate failures more easily than before in case of insufficient cold cranking capability.

Acknowledgements

The authors are indebted to Prof. Dr. H. Ewe, Technical University of Braunschweig, for the sorption experiments, and to Mr. E. Rosskopf, Varta Batterie AG, for his assistance in various experiments and mathematical calculations.

References

1 G. W. Vinal, Storage Batteries, Wiley, New York, 1955, p. 206.
2 W. Feitknecht, Ber. Buns. Phys. Chem., 62 (1958) 795.
3 J. P. Carr, N. A. Hampson and R. Taylor, J. Electroanalyt. Chem., 33 (1971) 109.
4 G. Archdale and J. A. Harrison, J. Electroanalyt. Chem., 34 (1972) 21; 47 (1974) 93.
5 M. P. J. Brennan and N. A. Hampson, J. Electroanalyt. Chem., 48 (1973) 465.
6 K. J. Vetter, Chem.-Ing. Techn., 45 (1973) 213.
7 A. Winsel, Ber. Buns. Phys. Chem., 79 (1975) 827.

Nomenclature

Δc maximum possible concentration gradient for supersaturation,
C capacity,
C_H high rate capacity,
f^* critical factor,
I current per unit weight of active material,
j current density ($j = I/S$),
$l(r)$ total length of pores with the radius r,

Δm	mol H_2SO_4/l of electrolyte of initial concentration c^0 which are consumed during discharge until the final electrolyte concentration c^1,
m^0	total amount of mol H_2SO_4 and H_2O/l of electrolyte of concentration c^0,
n	transport number,
$O(r)$	distribution function of the pore surface,
P^*	porosity of the diaphragm,
R_δ	resistance of the diaphragm,
r	pore radius,
R	internal surface calculated from pore volume distribution,
S	internal surface of active materials (BET surface),
t	time,
t^*	time until end of discharge,
$V(r)$	distribution function of the pore volume,
ΔV_0	volume change during charge/discharge,
V_P	pore volume of active materials,
x^0	mol fraction of H_2O in the electrolyte of concentration c^0,
x^1	mol fraction of H_2O in the electrolyte of concentration c^1,
y^0	mol fraction of H_2SO_4 in the electrolyte of concentration c^0,
y^1	mol fraction of H_2SO_4 in the electrolyte of concentration c^1,
δ	thickness of the diaphragm (passivation layer),
λ	tortuosity factor,
ρ	specific resistance of electrolyte solution,
θ	characteristic time,
τ	integration time variable,
κ	ratio of measured capacity and theoretically calculated C_H/C_{HV},
κ_∞	$1/(1 \pm n_-)$